Supplementary Information

Enhanced performance of dual-functional ZIF-8/RP photocatalyst for concurrent degradation of organic dyes and hydrogen generation under natural solar light irradiation

Shafali Singh and Sushil Kumar Kansal*

Dr. S. S. Bhatnagar University Institute of Chemical Engineering and Technology, Panjab University, Chandigarh-160014, India

*Corresponding Author: Prof. Sushil Kumar Kansal

Email id: sushilkk1@yahoo.co.in, sushilkk1@pu.ac.in

Keywords: Solar light; Photocatalytic degradation; Hydrogen generation; ZIF-8/RP heterostructure

Table S1. Comparison of the activity of ZIF-8/RP photocatalyst with other catalysts for the simultaneous photocatalytic degradation of organic pollutants and H_2 generation

Sr. No.	Catalyst	Application	Reaction conditions	Light source	Catalytic activity	Ref.
1.	Ni_2P QDs/red P nanosheets	Photocatalytic H_2 generation	Catalyst dose: 0.1 g/L Reaction mixture: 100 mL aqueous solution containing 10 vol% methanol	300 W Xe lamp ($\lambda \geq 420$ nm)	H_2 generation rate: 265.43 μmol·g^{-1}·h^{-1}	(1)
2.	TiO_2@RP heterostructure	Photocatalytic H_2 generation	Catalyst dose: 0.27 g/L Reaction Mixture: 150 mL distilled with added H_2PtCl_6 solution (3 wt.% Pt)	300 W Xe lamp ($\lambda >$ 300 nm)	H_2 generation rate: 215.5 μmol g^{-1}·h^{-1}	(2)
3.	Three-	Photocatalytic	H_2 generation	300 W Xe	H_2 generation	(3)

	dimensional structured kaolin/ red phosphorus composite photocatalyst	H_2 generation and degradation of RhB dye	experiments: Catalyst dose: 0.625 g/L Reaction mixture: 80 mL aqueous solution containing 10 vol% triethanolamine Degradation experiments: Catalyst dose: 0.25 g/L Pollutant concentration:10 mg/L Reaction time: 15 min	lamp	rate: 252 μmol h^{-1} g^{-1} Degradation efficiency: 98%	
4.	RP/MIL-101(Fe)	Degradation of tetracycline	Catalyst dose: 0.5 g/L Pollutant concentration:50 mg/L Reaction time: 80 min	300 W Xe lamp	Degradation efficiency: 90.1%	(4)
5.	ZIF-67/red phosphorus	Degradation of RhB	Catalyst dose: 1 g/L Pollutant concentration:20 mg/L Reaction time: 50 min	Visible light	Degradation efficiency: 98%	(5)
6.	WO_3/NiP_2 @ZIF-8	Photocatalytic H_2 generation	Catalyst dose: 0.33 g/L Reaction mixture: 30 mL of 30% triethanolamine and eosin-Y solution	5 W simulating visible light	H_2 generation rate: 295.7 μmol in 5h	(6)
7.	TiO_2@ZIF-8	Photocatalytic H_2 generation	Catalyst dose: 0.37 g/L Reaction mixture: 270 mL of methanol solution (20 vol%)	300 W Xe lamp	H_2 generation rate: 261.7 μmol g^{-1} h^{-1}	(7)
8.	ZIF-8/$BiFeO_3$	Degradation of RhB	Catalyst dose: 1 g/L	80 W visible light	Degradation efficiency:	(8)

			Pollutant concentration:10 mg/L Reaction time: 90 min		99.42%	
9.	AgBr@ZIF-8	Degradation of RhB	Catalyst dose: 0.5 g/L Pollutant concentration:10 mg/L Reaction time: 15 min	500 W Xe lamp	Degradation efficiency: 99.5%	(9)
10.	Ag/AgCl@ ZIF-8	Degradation of RhB	Catalyst dose: 0.5 g/L Pollutant concentration:10 mg/L Reaction time: 90 min	500 W Xe lamp	Degradation efficiency: 99.12%	(10)
11.	ZIF-8/Red phosphorus	Simultaneous photocatalytic degradation of RhB dye and H_2 generation	Catalyst dose: 0.4 g/L Reaction mixture: 50 mL aqueous solution containing 10 ppm RhB dye Reaction time: 4h	Natural sunlight	H_2 generation rate: 822.5 µmoles h^{-1} g^{-1} Degradation efficiency: 92%	**This work**

Experimental

Materials

All the analytical-grade reagents purchased for this work are commercially available and used without any modification. 2-methylimidazole ($C_4H_6N_2$, 99%), sodium hydroxide pellets (NaOH, 97%), hydrochloric acid (HCl, 36.5-38%), p-benzoquinone ($C_6H_4O_2$, 98%), isopropyl alcohol (C_3H_8O, 99%), potassium persulfate ($K_2S_2O_8$, 99%), ammonium oxalate ($(NH_4)_2C_2O_4$, 99%), methylene blue (MB), and malachite green (MG) were procured from Merck, India. Red phosphorus (RP, 98%), Zinc nitrate hexahydrate ($Zn(NO_3)_2 \cdot 6H_2O$, 98%), triethylamine ($C_6H_{15}N$, 98%), rhodamine B (RhB), and rhodamine 6G (Rh6G) were purchased from Loba Chemie Pvt. Ltd.-India. Ethanol (C_2H_6O, 99%) was procured from Sisco Research Laboratories

Pvt. Ltd. (SRL)-India. Double distilled water was utilized in all experiments and for the preparation of solutions.

Synthesis of pure RP and ZIF-8 MOF

Commercially available RP was hydrothermally treated at 200 ^{o}C for 12 h to remove the oxide layers. ZIF-8 MOF synthesis followed a solvothermal method outlined in prior study [11]. Briefly, 6.72 mmol of $Zn(NO_3)_2 \cdot 6H_2O$ was dissolved in 12 mL of double distilled water. At the same time, 40.43 mmol of 2-methylimidazole was dissolved in 48 mL of double distilled water followed by the addition of 2.5 mL of triethylamine solution. Then both the solutions were mixed and allowed to stir for 24 h. The resulting white product underwent thorough washing with ethanol and water mixture to remove any impurities. Finally, the white powder was obtained by drying the product overnight in an oven set at 80°C.

Synthesis of ZIF-8/RP heterostructures

ZIF-8/RP heterostructures were prepared using a solvothermal method. Briefly, to prepare 500 mg of ZIF-8/RP catalyst, 485 mg of RP was mixed in 50 mL of methanol solution under sonication. Similarly, 15 mg of as-prepared ZIF-8 MOF was dispersed in 50 mL methanol solution under sonication. Both the solutions were mixed and allowed for sonication to obtain a homogeneous suspension. Afterward, the obtained suspension was allowed to stir for 4 h and poured in a Teflon-lined autoclave, and put in a hot air oven for solvothermal treatment at 160 ^{o}C for 12 h. Now, the resulting product was cooled at room temperature and was centrifuged and washed several times using double-distilled water and ethanol mixture to remove the unwanted impurities. After washing, the final product was dried in a hot air oven at 80 ^{o}C overnight to obtain ZIF-8/RP heterostructures. During the synthesis, three different ZIF-8/RP heterostructures were prepared with different weight percentages of MOF in the heterostructure. Namely, three samples with 3 wt.% (ZRP-1), 5wt.% (ZRP-2), and 7 wt.% (ZRP-3) of ZIF-8 MOF in the ZIF-8/RP heterostructures were prepared using the similar procedure.

Characterization

XRD, FTIR, FESEM, HRTEM, Elemental Mapping, XPS, PL, UV-DRS, and EIS were used to characterize the prepared materials. On the Rigaku SmartLab SE diffractometer (Made in Japan), XRD patterns were collected in the 2θ range of 5-90^{o} at a scan rate of 10^{o} min^{-1} using an x'Celerator solid-state detector with Cu-Kα (λ = 1.54056 Å, 30 kV and 10 mA) radiation.

The appearance of various functional groups was examined using FTIR which was performed in the range of 400-4000 cm^{-1} on a Perkin Elmer-spectrum RX-I FTIR (Made in Canada) using KBr as a standard material. HRTEM images of the prepared samples were taken on JEOLJEM 2100 Plus (Made in Japan) high-resolution transmission electron microscope (HRTEM) equipped with a charge couple device (CCD) at 200 kV. The sample for HRTEM analysis was created by sonication of the material in ethanol, followed by drop-casting onto a carbon-coated copper grid, which was then air-dried. Using FESEM images on a Hitachi-SU 8010 Series (Made in Japan) at an accelerating voltage of 15 kV, the surface morphologies and elemental mapping of the prepared materials were examined. Before analysis, the sample was mounted onto an aluminum stub using carbon tape and subsequently coated with a thin layer of gold for 30 s. The elemental composition of the nanocomposite was determined using energy-dispersive X-ray spectroscopy (EDX) at an accelerating voltage of 15 kV. The sample for EDX analysis was prepared under similar conditions as for FESEM but without the application of a gold coating. The surface area was measured through N_2 adsorption-desorption isotherms using Quantachrome Autosorb IQ-XR-XR-XR (3 Stat.) Viton (Made in the USA). Before the surface area analysis, the samples were degassed at 150°C for 6 h. X-ray photoelectron spectroscopy (XPS, Thermo Fisher Scientific Escalab Xi+) (Made in the USA) with an ultra-high vacuum (UHV) system was used to study electronic states. The system included a monochromatic X-ray source (500 mm Rowland circle, Al anode), adjustable spot sizes (200 μm to 900 μm), magnetic immersion lens, 180° hemispherical energy analyzer (0-5,000 eV), and channel plate detectors for imaging. The six-channel electron multiplier detector was ideal for reflection electron energy loss spectroscopy (REELS) and ion scattering spectroscopy (ISS). The MAGCIS ion gun provided high-resolution depth profiling (100 eV to 4 keV). A high-resolution video camera with a field of view of 300 μm to ~2.5 mm ensured precise sample alignment. Photoluminescence analysis of the synthesized materials was conducted using a Hitachi F-7000 PL spectrophotometer (Made in Japan) (sensitivity (S/N 800:RMS) and ultra-high-speed (60,000 nm/min)). UV-vis absorption spectra were obtained with a Systronics 2202 spectrophotometer (200-1100 nm range, 2.0 nm bandwidth) (Made in India) in a quartz cuvette (1x1 cm, 4 mL). UV-vis diffuse reflectance spectra were measured using a Shimadzu UV-2600 spectrophotometer (Made in Japan) within the 200-800 nm wavelength range using $BaSO_4$ as a reflectance standard. Electrochemical impedance spectroscopy (EIS) was carried out using Potentiostat/Galvanostat equipment (Metrohm Multi Autolab/M204, Made in the Netherlands) with a 0.5 M Na_2SO_4 electrolyte. A maximum current of 10A can be obtained with the Booster 10A. The compliance voltage of the system was 20 V in combination with the Booster10A.

Mott-Schottky measurements were obtained at 1 kHz frequency under dark conditions. The transient photocurrent responses of samples using 0.5 M Na_2SO_4 electrolyte were recorded in the PGSTAT302N Autolab electrochemical system (Made in the Netherlands) with a 300 W Xe lamp, a maximum current of 2 A, with the option to increase to 20 A using the BOOSTER20A module and a current resolution of 30 fA at a 10 nA range. The pH of the solutions was maintained using a Mettler-Toledo FP 20 (Made in India) pH meter.

Evaluation of the photocatalytic activity of ZIF-8/RP heterostructures for degradation of organic dyes under solar light irradiation

The photocatalytic performance of the synthesized catalysts for degrading various organic dyes was evaluated outdoors under direct sunlight at the Dr. S. S. Bhatnagar University Institute of Chemical Engineering and Technology, Panjab University, Chandigarh-160014, India. The latitude and longitude coordinates of the location were 30.76° N and 76.77° E, respectively. The experiments were conducted in September and October, 2023 between 11:00 a.m. and 3:00 p.m. (IST), utilizing natural sunlight with an average light intensity of 80.5–85.0 mW/cm² over the 4 h reaction period. In each degradation trial, a certain quantity of catalyst was dispersed in 100 mL of aqueous solution containing organic dyes (10 mg/L). The mixture was then stirred in dark for a specified duration to establish adsorption/desorption equilibrium between the photocatalyst and pollutants. Following adsorption, the solution was exposed to solar light irradiation for 4 h. Throughout the experiments, samples of 2.5 mL were withdrawn at various time intervals using a syringe, then centrifuged to separate from the photolyzed reaction mixture.

Evaluation of the photocatalytic activity of ZIF-8/RP heterostructures for simultaneous degradation of organic dyes and H_2 generation under solar light irradiation

The photocatalytic activity of prepared photocatalysts for hydrogen generation was tested in a 100 mL borosilicate round bottom reaction flask. The experiments were carried out at the same location and the time frame that were used for the degradation experiments. Briefly, 0.02 g of the prepared photocatalysts were dispersed in a 50 mL solution of organic dyes of concentration of 10mg/L. After that, the reaction flask was purged with inert N_2 gas to remove the dissolved oxygen from the solution. Then, the reaction flask was completely sealed with septum and parafilm and kept in the dark to establish the adsorption/desorption equilibrium between the photocatalyst and pollutant. After adsorption, the solution was irradiated under solar light (average intensity 80.5–85.0 mW/cm^2) for 4 h for a photocatalytic water-splitting reaction.

Under solar light irradiation, the hydrogen produced in the reaction vessel will be collected using an airtight gas syringe and subsequently analyzed via NUCON 5765 gas chromatography (GC) (Made in India) employing a 5 Å sieve column and argon as the carrier gas, with detection facilitated by a thermal conductivity detector (TCD) (220 V, 50 Hz). Concurrently, the absorption spectra of organic dyes will be analyzed using a UV-vis spectrophotometer, and their respective degradation efficiencies will be calculated.

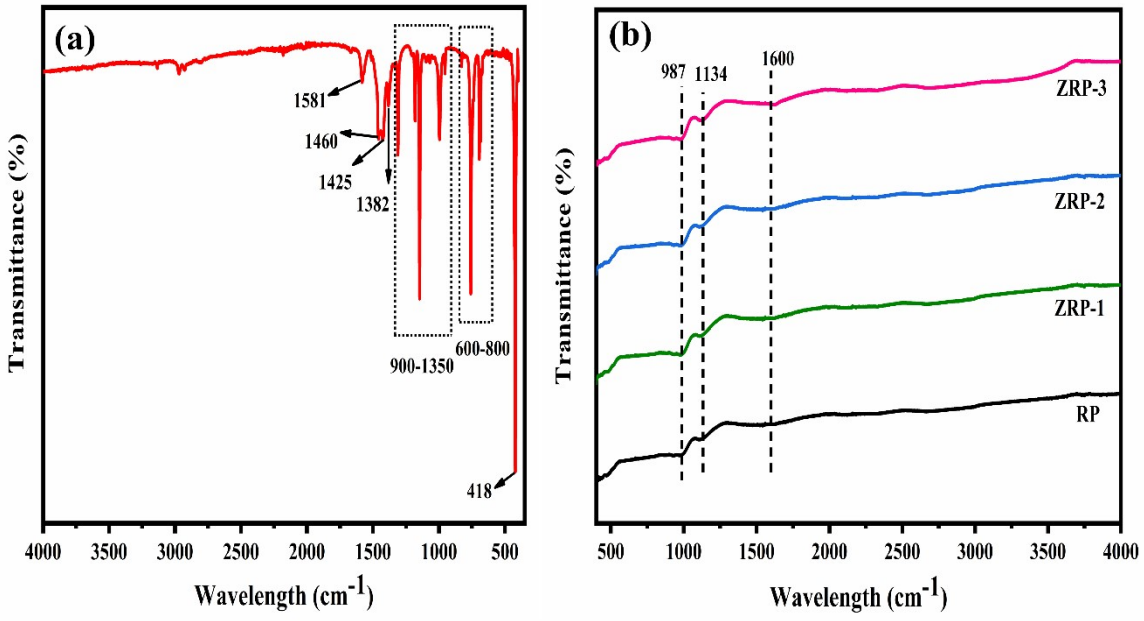

Fig. S1 FTIR spectra of (a) ZIF-8 and (b) ZIF-8/RP heterostructures

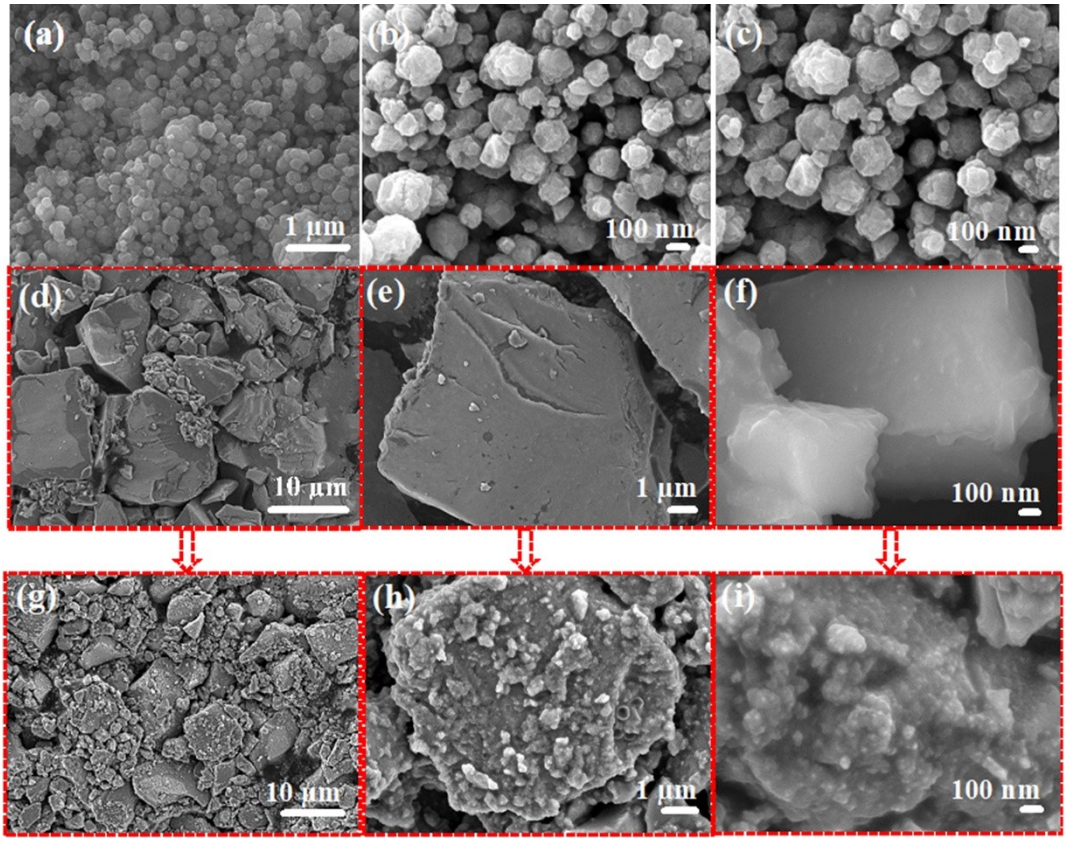

Fig S2 Morphological properties of (a-c) ZIF-8, (d-f) RP, and (g-i) ZRP-2

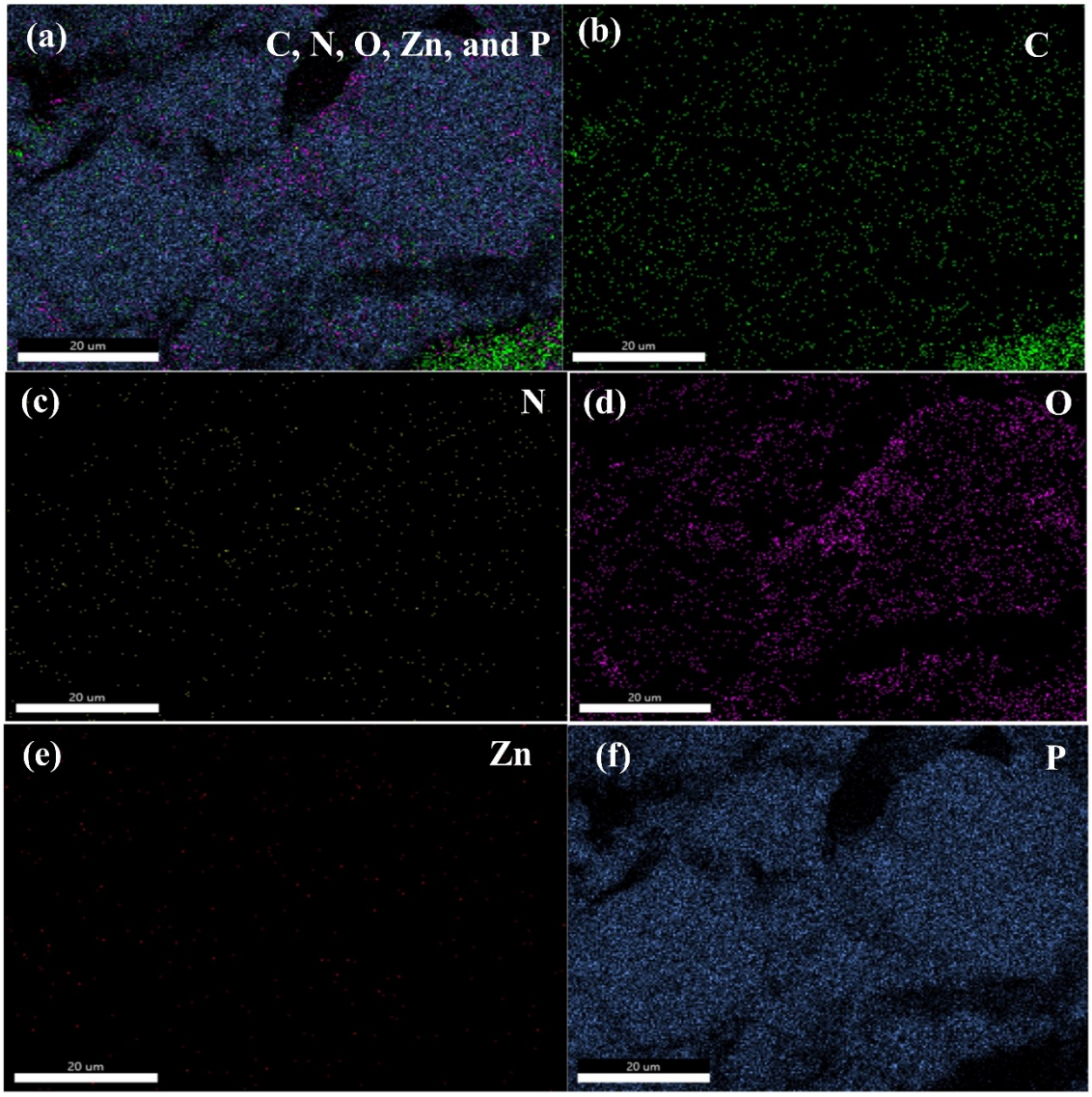

Fig. S3 Elemental mapping of ZRP-2

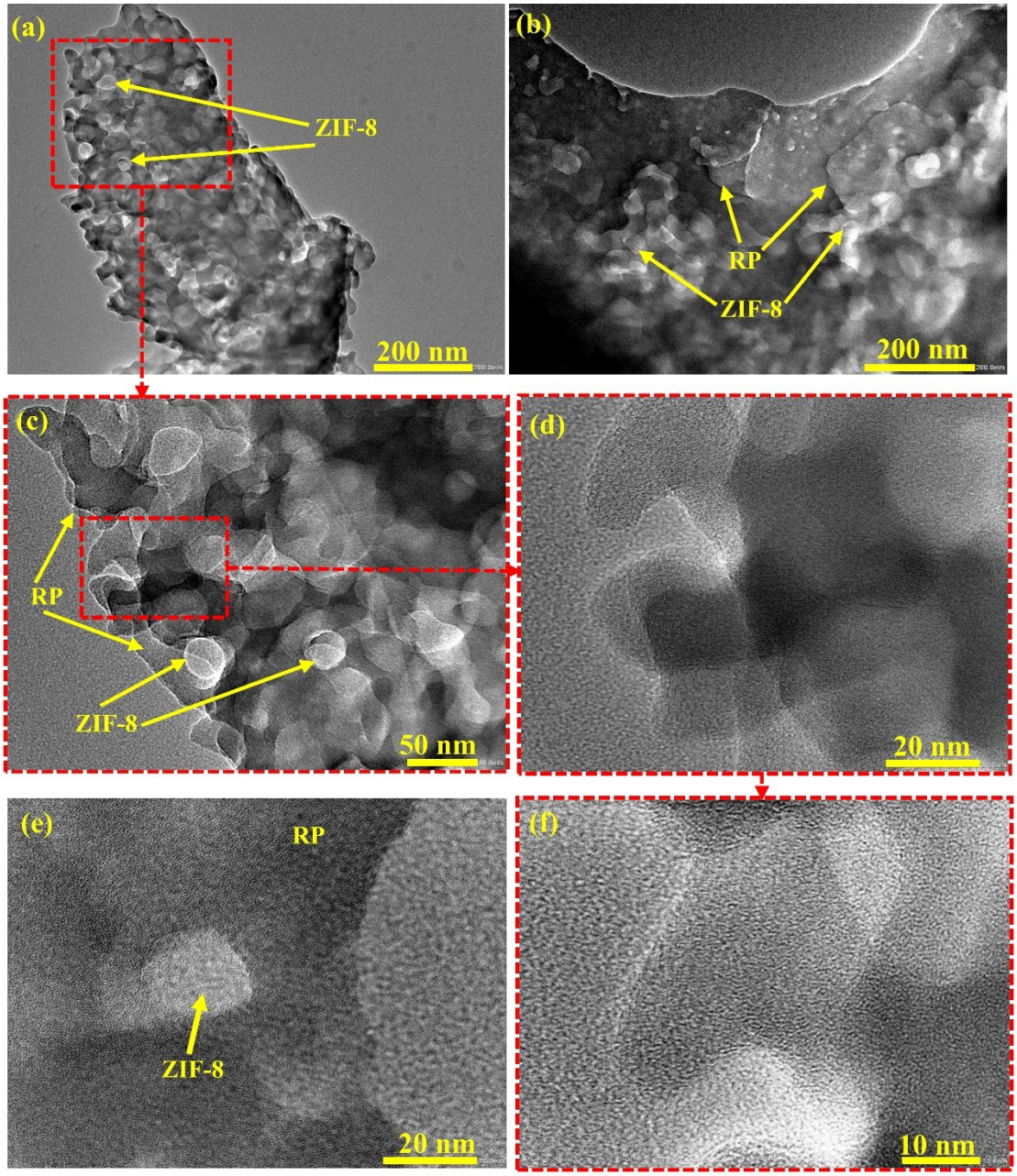

Fig. S4 HRTEM images of ZRP-2 catalyst

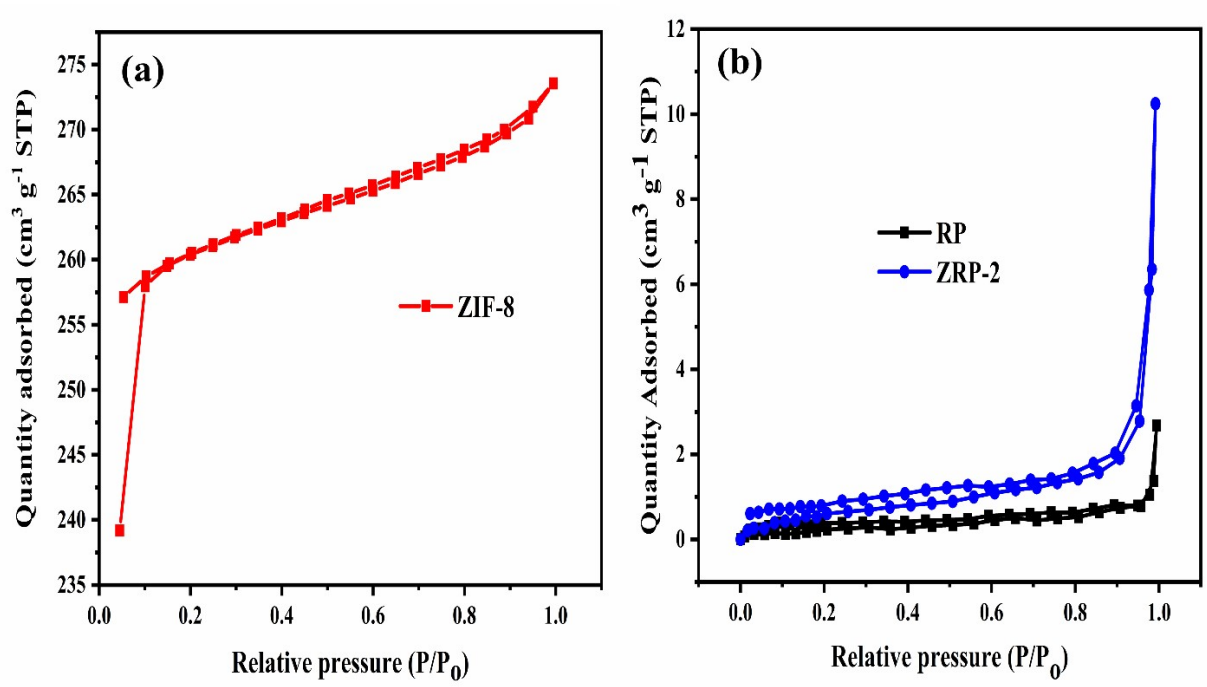

Fig. S5 N_2 adsorption-desorption isotherms of (a) ZIF-8 MOF and (b) RP and ZRP-2

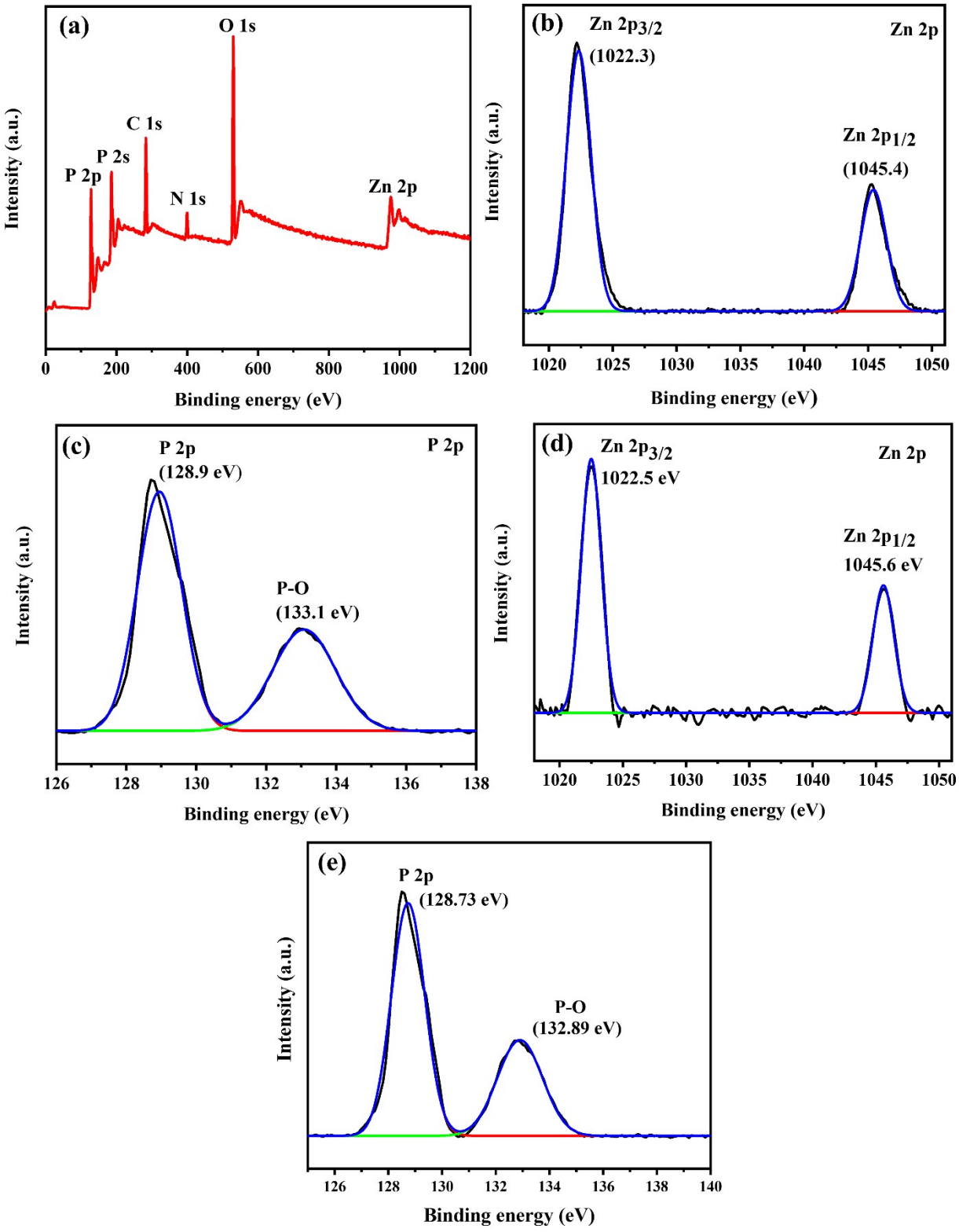

Fig. S6 Full survey XPS spectra of ZRP-2, XPS spectra of elements (b) Zn 2p of ZIF-8, (c) P 2p of bare RP, (d) Zn 2p of ZRP-2, and (e) P 2p of ZRP-2

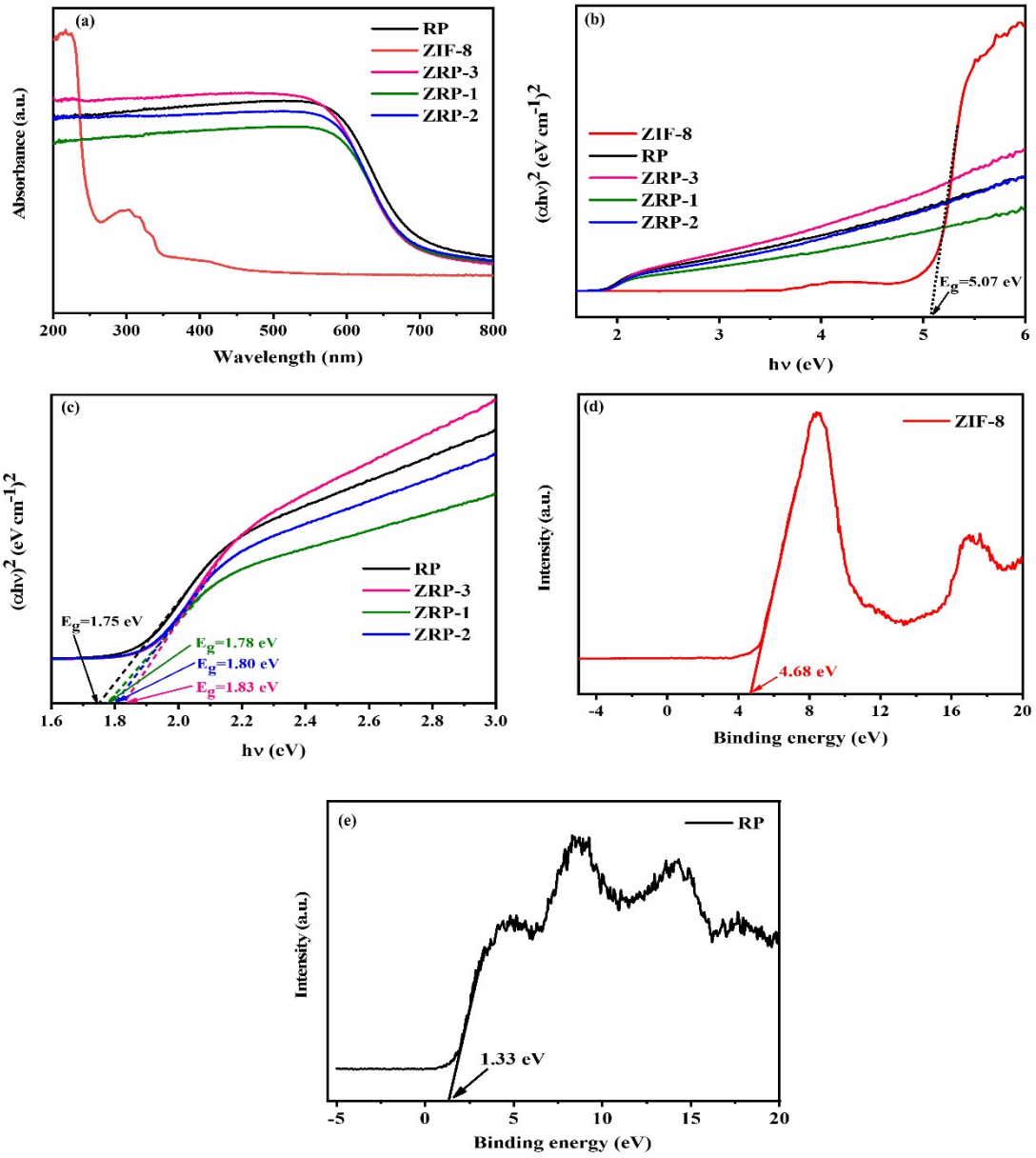

Fig. S7 (a) Absorbance of ZIF-8, RP, and ZIF-8/RP heterostructures, (b) Band gap energy of ZIF-8, (c) Band gap energies of ZIF-8, RP, and, ZIF-8/RP heterostructures, (d) VB XPS spectra of ZIF-8, and (e) VB XPS spectra of RP

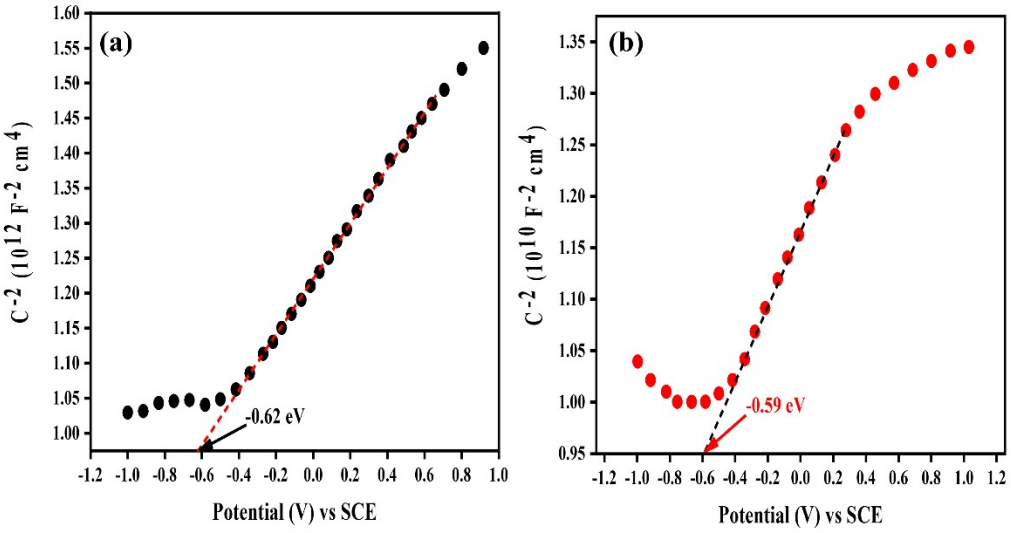

Fig. S8 Mott Schottky plots of (a) RP and (b) ZIF-8

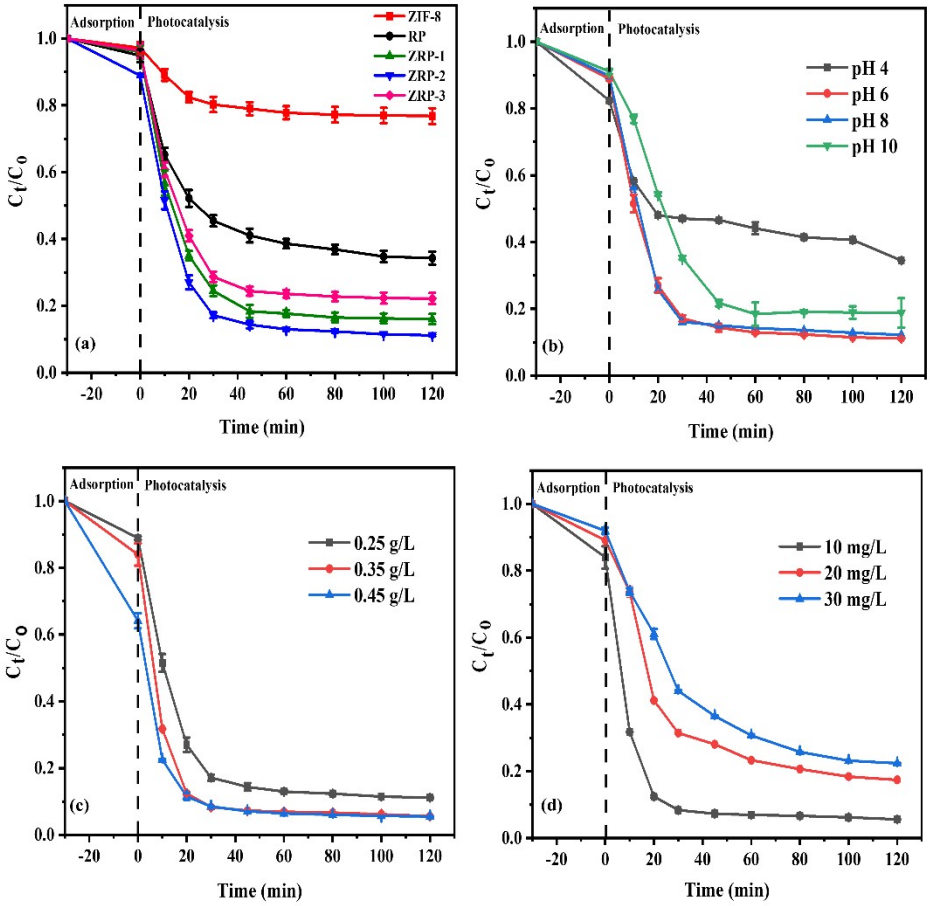

Fig. S9 (a) Degradation of RhB dye using prepared catalysts, Influence of (b) pH, (c) catalyst loading, and (d) RhB concentration on the photocatalytic activity of ZRP-2 catalyst

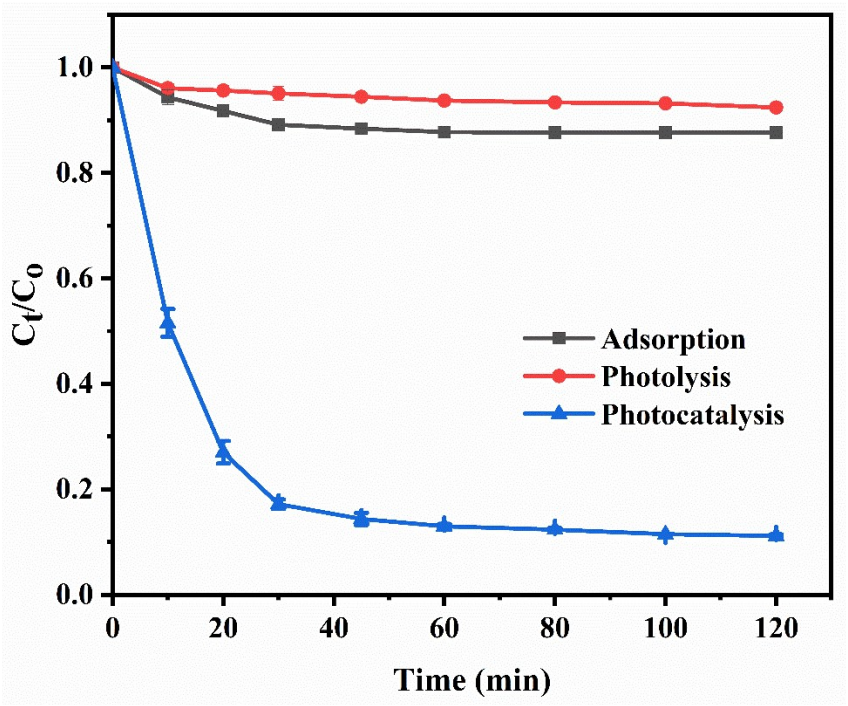

Fig. S10 Comparison of adsorption, photolysis, and photocatalysis for degradation of RhB dye using ZRP-2 catalyst

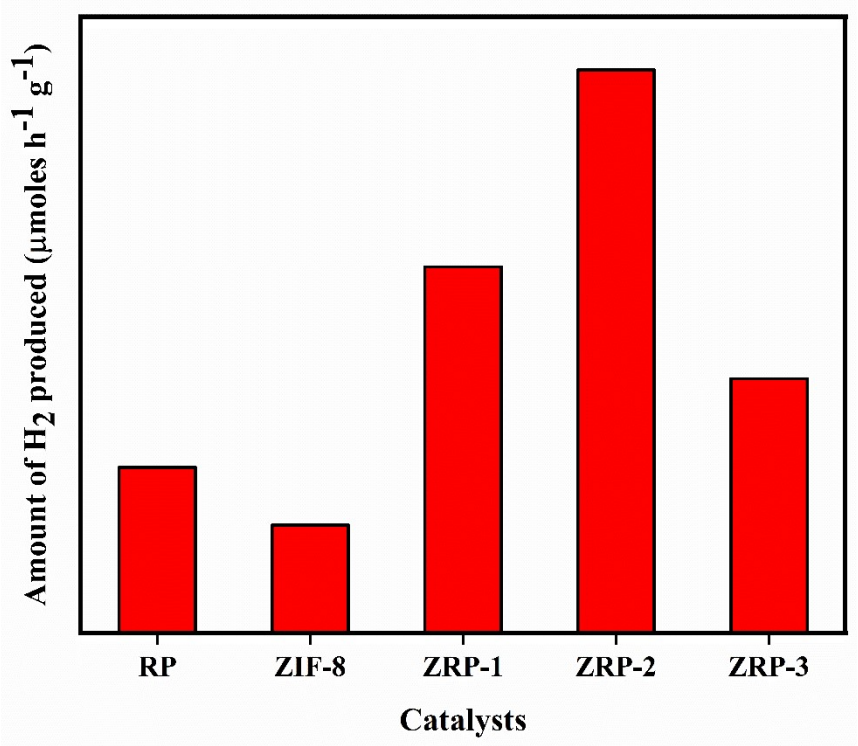

Fig. S11 Amount of H_2 generated in RhB dye solution using prepared catalysts under solar light irradiation

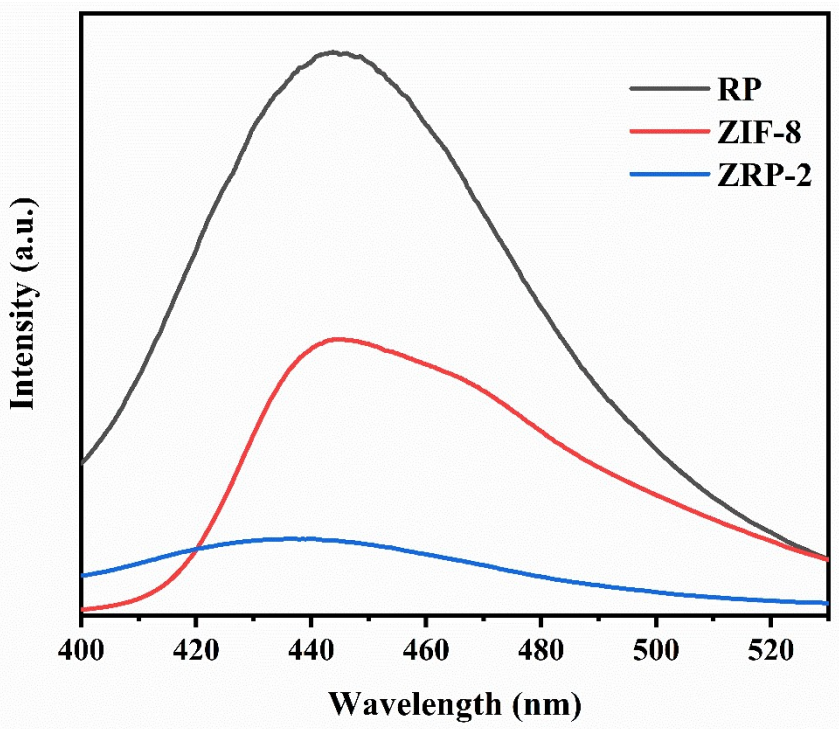

Fig. S12 PL emission spectra of RP, ZIF-8, and ZRP-2

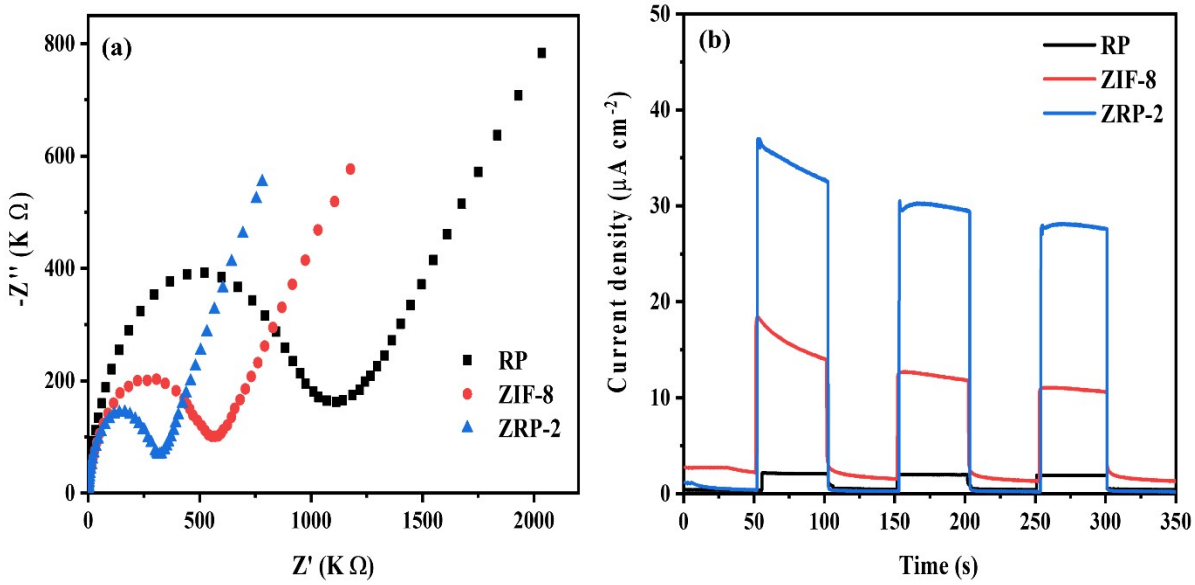

Fig. S13 (a) EIS and (b) Transient photocurrent response of RP, ZIF-8 and ZRP-2

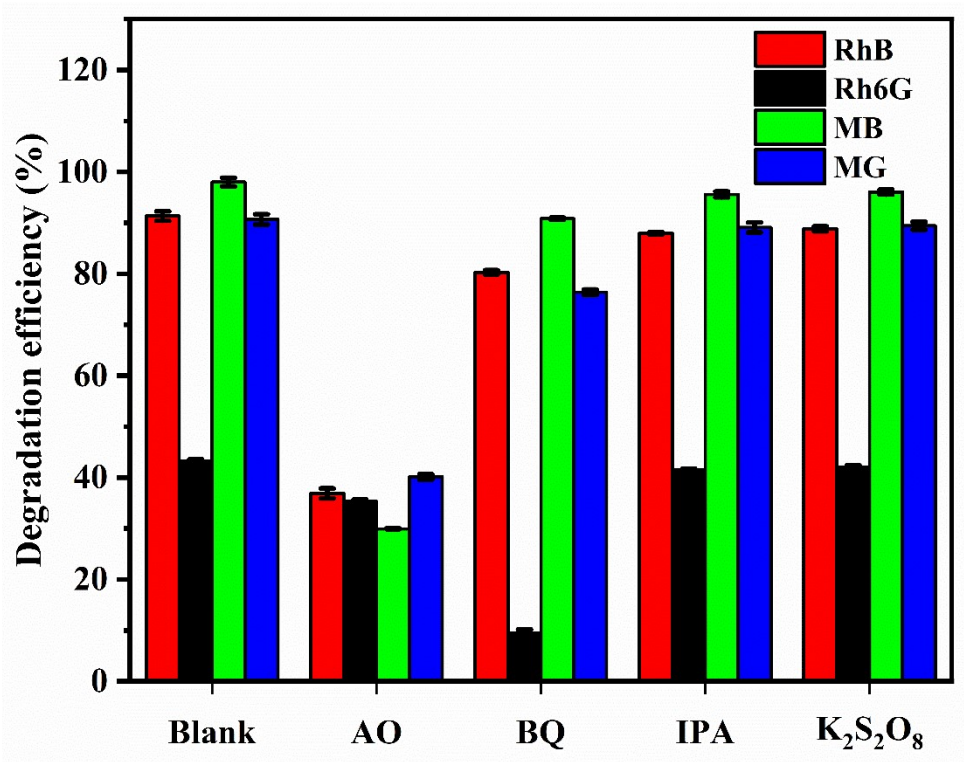

Fig. S14 Effect of scavengers on degradation of organic dyes over ZRP-2

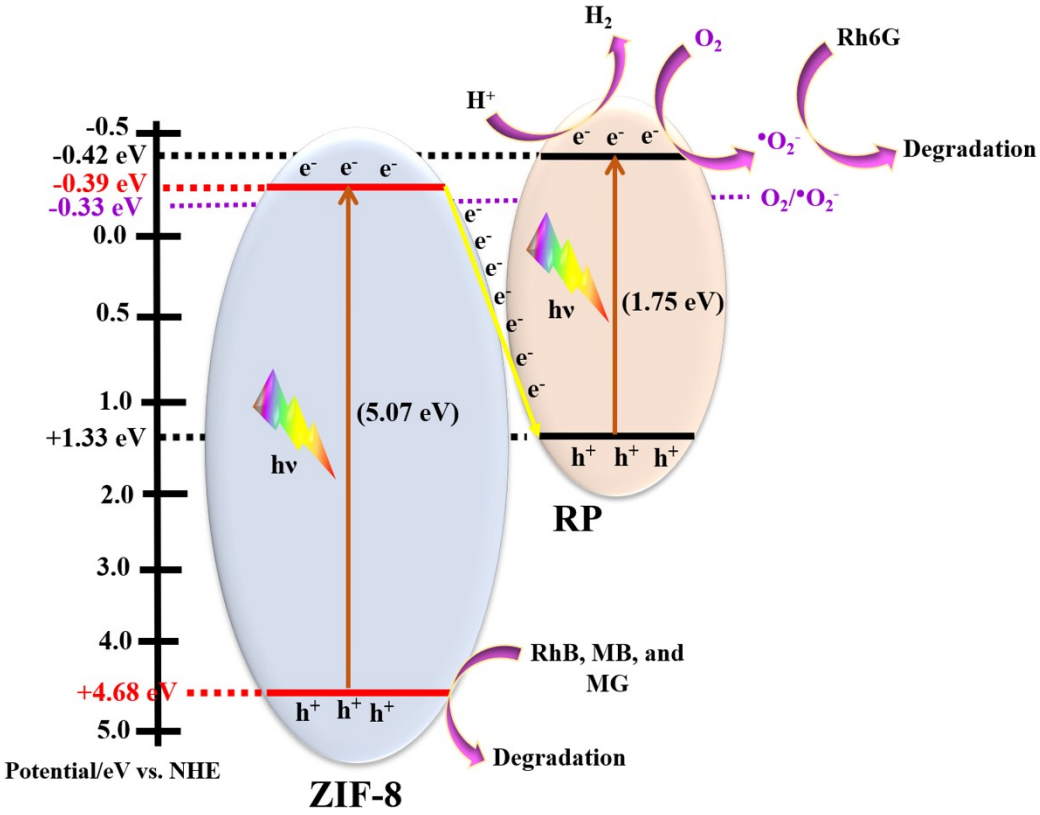

Fig. S15 Proposed photocatalytic mechanism of concurrent degradation of organic dyes and H_2 generation over ZRP-catalyst under natural sunlight irradiation

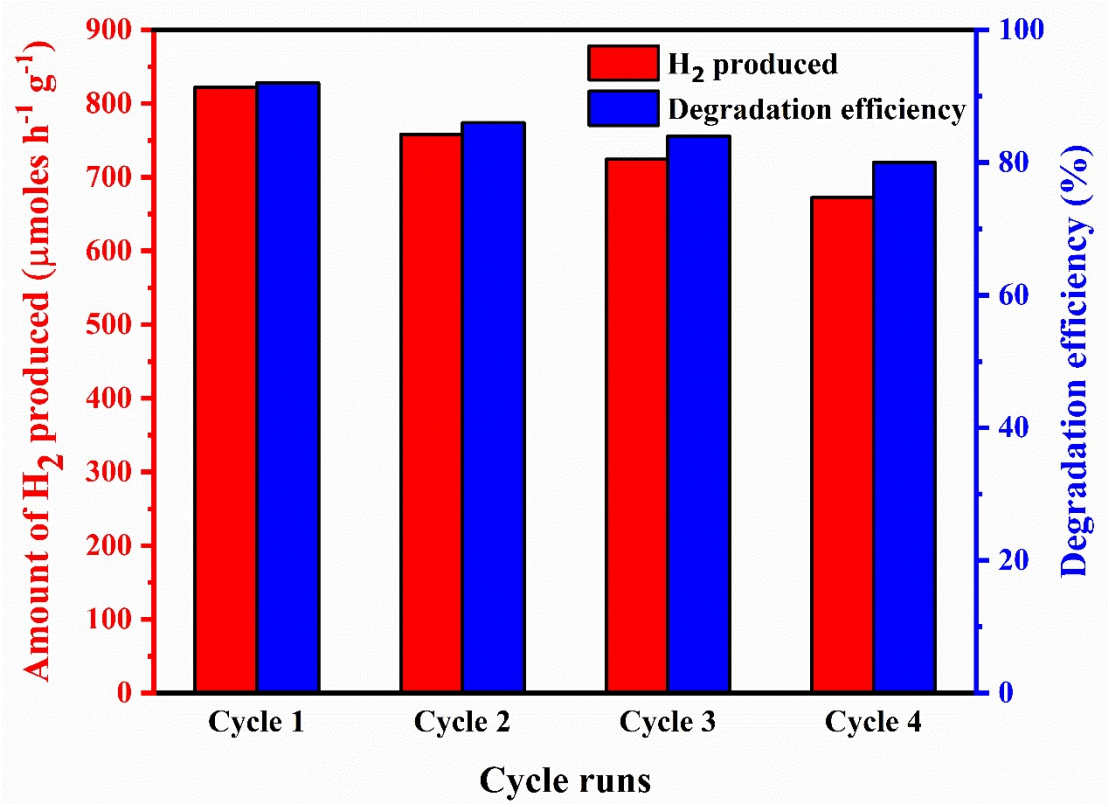

Fig. S16 Reusability of ZRP-2 catalyst for simultaneous degradation of RhB dye and H_2 production

Notes and references

1 Z. Liang, X. Dong, Y. Han and J. Geng, *Applied Surface Science*, 2019, **484**, 293–299.

2 G. Huang, W. Ye, C. Lv, D. S. Butenko, C. Yang, G. Zhang, P. Lu, Y. Xu, S. Zhang, H. Wang, Y. Zhu and D. Yang, *Journal of Materials Science & Technology*, 2022, **108**, 18–25.

3 C. Guo, H. Du, Y. Ma, K. Qi, E. Zhu, Z. Su, M. Huojiaaihemaiti and X. Wang, *Journal of Colloid and Interface Science*, 2021, **585**, 167–177.

4 X. Lei, J. Wang, Y. Shi, W. Yao, Q. Wu, Q. Wu and R. Zou, *Applied Surface Science*, 2020, **528**, 146963.

5 Y. Ma, D. Tuniyazi, M. Ainiwa and E. Zhu, *Materials Letters*, 2020, **262**, 127023.

6 Z. Jin and Y. Zhang, *Catalysis Surveys from Asia*, 2020, **24**, 59–69.

7 M. Zhang, Q. Shang, Y. Wan, Q. Cheng, G. Liao and Z. Pan, *Applied Catalysis B: Environmental*, 2019, **241**, 149–158.

8 B. Bethi, G. B. Radhika, L. M. Thang, S. H. Sonawane and G. Boczkaj, *Environmental Science and Pollution Research*, 2023, **30**, 25532–25545.

9 Y. Chen, S. Pu, D. Wang, Y. Zhang, G. Wan, Q. Zhao and Y. Sun, *Journal of Solid State Chemistry*, 2023, **321**, 123857.

10 G. Zuo, A. Wang, Y. Yang, H. Huang, F. Wang, H. Jiang, L. Zhang and Y. Zheng, *Journal of Porous Materials*, 2020, **27**, 339–345.

11 N. A. H. M. Nordin, A. F. Ismail, A. Mustafa, P. S. Goh, D. Rana and T. Matsuura, *RSC Advances*, 2014, **4**, 33292–33300.